Improving the Ordering and Photovoltaic Properties by Extending π–Conjugated Area of Electron-Donating Units in Polymers with D-A Structure

Ye Huang, Xia Guo, Feng Liu, Lijun Huo, Yuning Chen, Thomas P. Russell, Charles C. Han, Yongfang Li,* and Jianhui Hou**

Photovoltaic performance of polymer-based organic photovoltaics (OPVs) has improved greatly over the years, leading to a power conversion efficiency (PCE) of about 8% recently.[1–7] The bulk-heterojuction (BHJ) structure has proven to be the most successful structure for OPVs, where the active layer consists of a nanoscale bicontinuous phase-separated morphology of *p*-type and *n*-type materials.[8] Conjugated polymers are used as *p*-type materials in the active layer, which absorbs light and generates excitons that diffuse to the interface of the domains, where they are split into electrons and holes that are transmitted to the cathode and anode through their respective domains. The molecular design of new conjugated polymers is one of the most important, though challenging topics in OPVs. Most efforts have focused on conjugated polymers with alternating electron-rich (donor) and electron-deficient (acceptor) units, known as D-A structured polymers,[9,10] to tune their bandgaps and energy levels by controlling the intramolecular charge transfer (ICT) from the donor to the acceptor units or introducing electron-withdrawing side chains on the conjugated polymers to down-shift the HOMO level of the polymer.[11] For instance, significant progress has been achieved by decreasing the HOMO levels of the **PBDTTT**-based conjugated polymers through the introduction of carboxyl and fluorine to the acceptor thieno[3,4-*b*]thiophene (TT) unit, resulting in a higher V_{oc} and PCE.[2,12,13]

Y. Huang, X. Guo, Prof. L. Huo, Y. Chen, Prof. C. C. Han, Prof. J. Hou
State Key Laboratory of Polymer Physics and Chemistry
Beijing National Laboratory for Molecular Sciences
Institute of Chemistry,
Chinese Academy of Sciences
Beijing 100190, China
E-mail: hjhzlz@iccas.ac.cn

Prof. Y. Li
CAS Key Laboratory of Organic Solids
Institute of Chemistry
Chinese Academy of Sciences
Beijing 100190, China
E-mail: liyf@iccas.ac.cn

F. Liu, Prof. T. P. Russell
Department of Polymer Science and Engineering
University of Massachusetts
Amherst, Massachusetts 01003, USA
E-mail: russell@mail.pse.umass.edu

DOI: 10.1002/adma.201200995

Although there have been many routes developed to tailor the energy levels and bandgaps by modifying the molecular structure, there is an urgent need to correlate the molecular structure with the morphology of these polymers. Understanding the morphology, the interactions between the polymer and the electron acceptor (typically a PCBM-based material), and the ordering of the polymer itself are the key to further improvement of the BHJ OPV performance. The morphology of the active layer is usually controlled by various processing conditions, such as the solvent casting conditions, thermal and solvent annealing, the use of processing additives, and the substrates used. For instance, thermal annealing has been employed in P3HT system to optimize the morphology and achieve high efficiencies.[14] Additives have been successfully applied to control the nanoscale morphology, so as to enhance efficiency.[15,16] While these studies demonstrate the importance of the structural ordering and morphology, the chemical structure of the polymer will also influence the intra- and intermolecular ordering of the polymers. For example, a planar conjugated backbone and efficient intermolecular packing of the polymer are obtained by replacing the bulky ethylhexyl side chains with a less bulky octyl side chain in *N*-alkylthieno[3,4-*c*]pyrrole-4,6-dione (TPD) based polymer,[17] while the π–π stacking property can be enhanced by replacing the carbon atom with a silicon atom to reduce steric hindrance.[18,19]

Understanding the correlation between the molecular structure, morphology and photovoltaic properties of conjugated polymers used in bulk heterojunction (BHJ) polymer-based, organic photovoltaics (OPVs) is of critical importance in designing high-efficiency organic photovoltaic polymers. With these criteria in mind, we have taken a systematic and effective molecular design route to control and tune the structural ordering and morphology of new low bandgap polymers and their blends with [6,6]-phenyl C_{71}-butyric acid methyl ester ($PC_{70}BM$). Here, we focus on using molecular modifications to achieve optimized thin film morphologies and, therefore, high efficiencies. Poly[(2-((2-ethylhexyl)sulfonyl)thieno[3,-*b*]thiophen-2,6-diyl)-*alt*-(4,8-bis(2-ethylhexyloxy)benzo[1,2-*b*:4,5-*b*']dithiophene)-2,6-diyl] (**PBDTTT-S**), a polymer based on benzo[1,2- b:4,5-*b*']dithiophene (BDT) and thieno[3,4-*b*] thiophene (TT), was chosen, since it has bulky sulfonyl side group that results in a disordered packing of the chains. Based on the strategy of achieving conjugated polymers with large π-overlap area and good ordering structure, here we report one

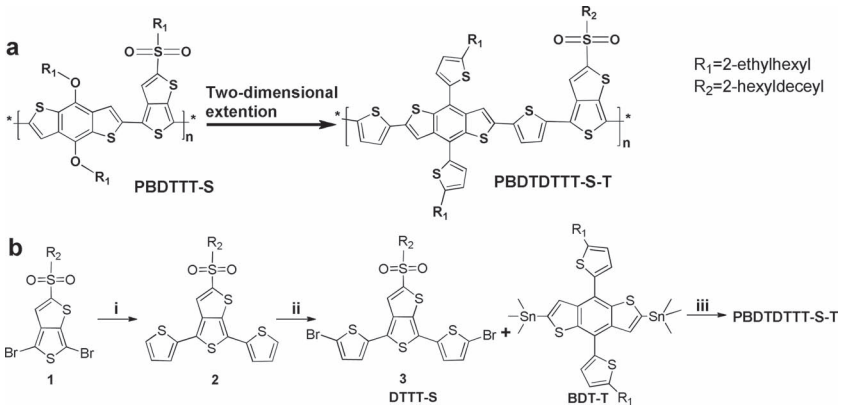

Scheme 1. a) Molecular design Route of the polymers: **PBDTTT-S** and **PBDTDTTT-S-T.** b) Synthetic Routes of monomer DTTT-S and polymer **PBDTDTTT-S-T**: (i) tributyl(2-thienyl) stannane, Toluene, DMF and $Pd(PPh_3)_4$, 110 °C; (ii) NBS, DMF, argon, 0 °C; (iii) $Pd(PPh_3)_4$, toluene, DMF, 110 °C, 13 h, argon.

new polymer, poly[(((2-hexyldecyl)sulfonyl)-4,6-di(thiophen-2-yl)thieno[3,4-*b*]thiophene-2,6-diyl)-alt-(4,8-bis((2-ethylhexyl)oxy)benzo[1,2-*b*:4,5-*b*']dithiophene-2,6-diyl)] (**PBDTDTTT-S-T)**, where T represents the thiophene side group on the BDT unit. (See **Scheme 1**) Introducing the thiophene unit onto the BDT side position and between the BDT-T and TT-S units can enlarge the π-overlap area parallel to and normal to the chain axis and reduce the steric hindrance between side chains. Grazing Incidence X-ray Diffraction (GIXD) shows that the extent of two-dimensional ordering is enhanced by enlarging the conjugated area of donor unit and reducing steric hindrance of the sulfonyl group. Compared with **PBDTTT-S**, **PBDTDTTT-S-T** exhibits high hole mobility and PCE. The photovoltaic performance based on **PBDTDTTT-S-T** shows a V_{oc} of 0.69 V, a J_{sc} of 17.07 mA/cm^2, and a *FF* of 66.3%, leading to an efficiency of 7.81%. Consequently, extending the conjugated area represents a promising approach to modify the morphology of the active layer in PSCs and to improve device performance.

In our recent work on the **PBDTTT-S**,[13] the sulfonyl group was used to decrease the HOMO level and enhance the V_{oc}, due to its strong electron-withdrawing ability. The resulting polymer **PBDTTT-S** shows a V_{oc} of 0.76 V, but the FF and J_{sc} of the **PBDTTT-S**-based device are lower than those of other **PBDTTT**-based polymers. Density functional theory (DFT) calculations were used to predict the geometry of the repeating unit. These calculations indicated that the sulfonyl bond angle is about ~ 108°, (see Figure S1 in Supporting Information), which blocks the interchain π-π stacking of **PBDTTT-S**, leading to reduced carrier mobility. Consequently, molecular design was targeted to improve the π-overlap area between adjacent chains, so as to enhance photovoltaic properties. Previous research on discotic liquid crystals showed that increasing the mesogen core, which increases the π-π co-facial overlapping, could enhance the interplanar electronic interactions, thereby leading to an increased mobility.[20,21] For this purpose, a thiophene side chain was introduced into the BDT unit to increase the conjugated area. Another effective route is to reduce the content of the bulky side groups in the polymer or increase the distance between sulfonyl and thiophene side groups. Therefore, we introduced two thiophene units adjacent to the BDT. The introduction of the five-membered ring into the conjugated backbone usually results in a small torsional angle[22] and reduced steric hindrance, so a more planner main chain structure could be expected, that could lead to improved interchain interactions and mobility.[23,24] While TT-S and BDT-T were synthesized by procedures described in the literature,[1,13] the synthesis of the monomer DTTT-S is shown in Scheme 1b. All these polymers exhibited good thermal stability, showing less than 5% weight loss at temperatures up to 350 °C, which is adequate for the fabrication processes for OPVs and other optoelectronic device applications.

All polymers exhibited nearly identical absorption while there was a slight difference in the absorption edges of their thin films (**Figure 1**a and see solution absorption spectra in Supporting Information). For **PBDTTT-S**, the absorption edge at 750 nm in the solid film corresponds to an optical bandgap of 1.65 eV. While for **PBDTDTTT-S-T**, the absorption spectra red-shifted by about 20 nm in the thin film, as their absorption edges are located at 780 nm, corresponding to an optical bandgap of 1.59 eV. It is important to note that the solid state absorption profiles are much boarder than the solution spectra, which is an interesting feature for OPV applications.

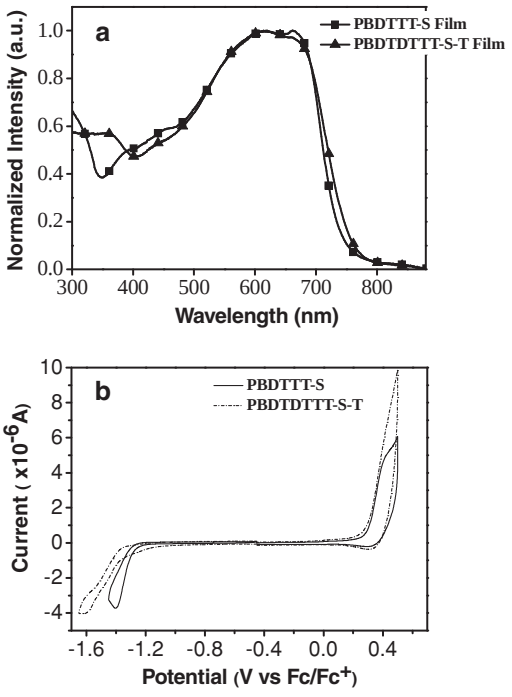

Figure 1. a) Normalized UV-vis absorption spectra of **PBDTTT-S** and **PBDTDTTT-S-T** in solid films on quartz. b) Cyclic voltammograms of their films on a platinum electrode in 0.1 M Bu_4NPF_6, CH_3CN solution. The ferrocene/ferrocenium redox couple is used as a standard (-4.8 eV).

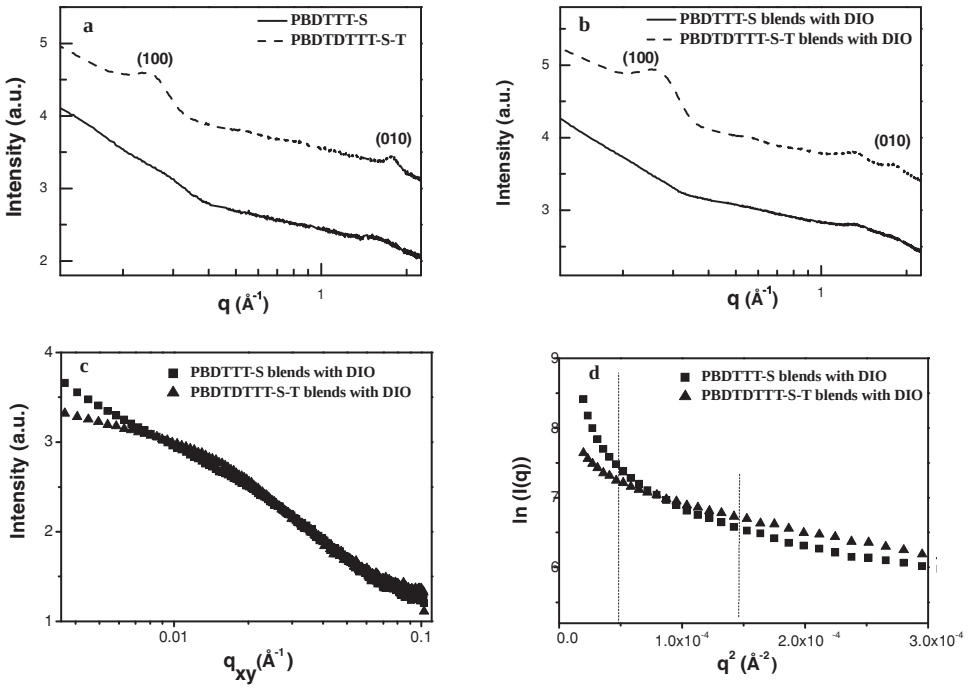

Figure 2. The out-of-plane GIXD curves for a) pure thin films, b) blends films of **PBDTTT-S** and **PBDTDTTT-S-T** with $PC_{70}BM$ and DIO (These curves were taken in a direction normal to the substrate.) and c, d) In-plane GISAXS curves for blends films of **PBDTTT-S** and **PBDTDTTT-S-T** with $PC_{70}BM$ (These curves were taken from the direction parallel to the substrate). Incidence angles at 0.20°. (The blends film compositions and preparations were consistent with those generally used in optimized solar cells).

Cyclic voltammetry (CV) was used to measure oxidation and reduction potentials of the polymers (Figure 1b). **PBDTTT-S** presents one irreversible *p*-doping (with onset oxidation potential E_{ox} = 0.30 V vs. Fc/Fc^+) process and one irreversible *n*-doping (with onset reduction potential E_{red} = −1.29 V vs. Fc/Fc^+). The HOMO and LUMO levels of the polymers were calculated from the electrochemical onset oxidation potential (E_{ox}) and the onset reduction potential (E_{red}), respectively, where HOMO = −e(E_{ox} + 4.80) (eV) and LUMO = −e(E_{red} + 4.80) (eV).[25] Extending the conjugation of electron-donating units parallel to the back-bone elevated the HOMO level of **PBDTDTTT-S-T** by ~0.06 eV, which will decrease the V_{oc}, since the V_{oc} is correlated with the difference between the HOMO level of the electron donor and the LUMO level of the electron acceptor.[26]

The D-A structured polymers allow the π-electron conjugation to extend all the way across the main conjugated chain. To gain insight into the electronic properties of these polymers, computations were performed using density functional theory (DFT). The electronic density distributions of the HOMO and LUMO of the oligomers (three repeating units) are shown in Figure S3 in Supporting Information. The HOMOs and LUMOs are well delocalized over the whole conjugated chain due to the quinoid structure of TT unit.[27] The thiophene bridge between the donor and acceptor can increase the distance between thiophene side group and sulfonyl side groups and, therefore, reduce the steric interference and achieve good π-π stacking and interchain ordering (shown in GIXD data later).

GIXD has been widely used to characterize the formation of ordered structures within thin films. In this study, this technique is used to examine the crystalline structure of the pure polymers and their blends with $PC_{70}BM$ and 1,8-diiodooctane (DIO). **Figure 2**a shows the out-of-plane GIXD profile of a spin-coated **PBDTTT-S** film from an *o*-dichlororbenzene (DCB) solution. For **PBDTTT-S** sample, a quite weak broad peak at ~0.29 $Å^{-1}$ was observed (corresponding to a d-spacing of 21.6 Å), indicating that the crystallinity of this polymer is quite low. Directly introducing the thiophene side chains into the BDT unit makes the polymer chain quite crowded, which hampers the side chain interdigitation or organization, thus reducing the overall order of the polymer chains. This effect can be relieved by introducing spacer thiophene rings in the main chain. The resulting polymer **PBDTDTTT-S-T** shows a pronounced (100) reflection at 0.26 $Å^{-1}$, corresponding to a d-spacing of 24.2 Å. The increased (100) d-spacing is due to the long alkyl chain used in the sulfonyl group to ensure solubility and processability of the polymer. A reflection was also observed at 1.79 $Å^{-1}$ which corresponds to the (010) π-π stacking packing. These results indicate that **PBDTDTTT-S-T** adopts a mixed face-on and edge-on orientation in the thin film. It is interesting to note that the d-spacing for this π-π stacking is calculated to be 3.51 Å, which is the smallest π-π stacking distance for conjugated polymers to the best of our knowledge. In comparison to **PBDTTT-S**, which has quite weak reflection at 1.62 $Å^{-1}$, corresponding to the π-π stacking with d-spacing of 3.88 Å, a large reduction of stacking distance for **PBDTDTTT-S-T** is found, which is consistent with the material design protocol, i.e. by increasing the π-conjugation area, the interchain interactions are enhanced.

When the polymers are blended with $PC_{70}BM$, the structural order of polymer is usually disturbed due to the miscibility of the two components.[28] The processing conditions are also

known to strongly affect the morphology of the blends. These details were also examined here. To give a better correlation between morphology and device function, the blended samples are prepared according to standard device fabrication procedures. A thin layer of PEDOT:PSS, spin coated onto a Si wafer, was used as the substrate to investigate the morphology of the blends. The polymer and $PC_{70}BM$ were dissolved in DCB and a ~100 nm thick film was spin-coated on top of the PEDOT:PSS to investigate the morphology. For **PBDTTT-S**, the scattering profiles were similar to those of the pure polymers, with the $PC_{70}BM$ reflection at 1.36 A^{-1}. Marked changes occurred in the case of the **PBDTDTTT-S-T**:$PC_{70}BM$ blends. The previously well-defined crystalline reflections of **PBDTDTTT-S-T** disappeared and no $PC_{70}BM$ was observed (see Figure S4 of GISAXS results and Figure S5 of device results in Supporting Information). Consequently, the $PC_{70}BM$ disrupted the ordering of the polymer.

Since additives can strongly affect the morphology of mixtures of low bandgap polymers with PCBM, 3 v% of DIO was added to the DCB solution of the blends prior to spin coating. The addition of the DIO was found to significantly enhance the device performance. Shown in Figure 2b are the GIXD profiles of thin films of polymer:$PC_{70}BM$ blends with DIO. In the case of **PBDTTT-S**, the ordering of the polymer was found to be even better than that of the pure polymer. This is similar to the results of Kramer and coworkers[29], Nelson and coworkers[30] and Russell and coworkers[31] with PCPDTBT. For **PBDTDTTT-S-T**, with the addition of DIO, the structural order of the polymer recovered, similar to that observed in a polymer thin film. Both (100) and (010) peaks were observed. The full width at half maximum (FWHM) for the (100) peak was 0.098 $Å^{-1}$, which corresponds to a persistence of the ordering along the (100) direction of 6.4 nm. The FWHM for the (010) peak is 0.12 $Å^{-1}$, which gives a persistence of the ordering along the (010) direction of 5 nm. These values are much smaller than that found for P3HT:PCBM blends.[28]

Figure 2c shows the grazing incidence small angle X-ray scattering, GISAXS, profiles of the polymer:fullerene blends prepared with DIO. **PBDTTT-S** shows a very weak reflection at ~0.015 A^{-1}, corresponding to a center-to-center distance between adjacent domains of ~21 nm. However, for **PBDTDTTT-S-T**:$PC_{70}BM$ blends, a distinct interference at 0.02 A^{-1}, corresponding to a center-to-center distance between adjacent domains of ~15 nm, was observed, characteristic of a phase separated morphology.

Guinier's Law, $I(q) = I(0)\exp(-R_g^2q^2/3)$ in which R_g is the radius of gyration of scatterers, $I(q)$ is the scattering intensity, q is the scattering vector, and $I(0)$ is the zero angle scattering intensity, was used to estimate the average size of the domains. Figure 2d shows a plot of $\ln(I(q))\sim q^2$ where, from the slope, R_g^2 can be determined. The low q range (0.006-0.012 A^{-1}) was used to determine the R_gs for **PBDTTT-S** and **PBDTDTTT-S-T**, which were 16 and 12 nm, respectively, and are commensurate with exciton diffusion length and appropriate for OPV application.

Transmission Electron Microscopy (TEM) was used to obtain a real space image of the phase separated morphology of the polymer-fullerene blends. As we can see in **Figure 3**, **PBDTTT-S**/$PC_{70}BM$ blends give a homogeneous morphology, while **PBDTDTTT-S-T**/$PC_{70}BM$ blends, though, show the formation of nanoscopic fibrils that permeate the film, suggesting that the ordering has been markedly improved.[32] From the results shown, it is evident that the DIO additive has promoted the demixing of the polymer and PCBM and has induced the fibril formation, leading to the final morphology shown in Figure 3b. From studies on other low bandgap systems it would be expected that the interfibrillar regions are comprised of crystalline domains of **PBDTDTTT-S-T** with PCBM being forced into the intercrystalline areas. Atomic force microscopy (AFM) was employed to characterize the surface morphology of the thin film blends (shown in Figure 3). Figure 3c and 3d show the typical height and phase images of blend films whose preparation conditions were kept the same as those in the device

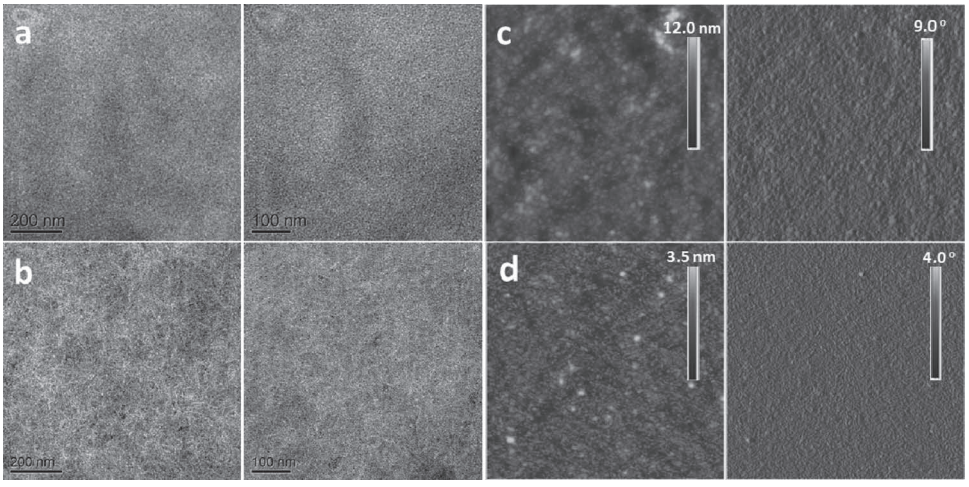

Figure 3. a) TEM images and c) AFM images of **PBDTTT-S**:$PC_{70}BM$ (1:1.5, w/w) and containing 3 vol% of DIO, b) TEM images and d) AFM images of **PBDTDTTT-S-T**:$PC_{70}BM$ (1:1, w/w) and containing 3 vol% of DIO, respectively. The scales in TEM are 200 nm (left) and 100 nm (right). AFM images: left are height images and right are phase images (All the images are 2 μm × 2 μm.).

Table 1. Basic Properties (Optical and Electrochemical) and Hole Mobilities of the Polymers Measured by Space-Charge-Limited Current (SCLC) Method.

POLYMER	E_g^{opt} [eV]	HOMO [eV]	LUMO [eV]	DFT calculated HOMO [eV]	Hole Mobility [$cm^2V^{-1}s^{-1}$]
PBDTTT-S	1.65	−5.10	−3.51	−5.08	4.56×10^{-4}
PBDTDTTT-S-T	1.59	−5.04	−3.57	−4.83	2.76×10^{-3}

fabrication. The surface of **PBDTDTTT-S-T** blend film is significantly smoother than that of **PBDTTT-S** blend film, with root-mean-squared surface roughness of 0.74 nm (Figure 3d) compared to 3.29 nm (Figure 3c).

The hole mobilities, μ_{hole}, of the blends of polymers and $PC_{70}BM$ were measured using the space-charge-limited current (SCLC) method (**Table 1**).[33,34] The strong π-π stacking of the planar polymer backbone has been a key structural feature of many semiconductors with high charge-carrier mobility. The mobility obtained with **PBDTDTTT-S-T** was approximately one order higher than that of **PBDTTT-S**. In particular, the appended carbon bond on the sulfonyl group has a ~108° bond angle with respect to the conjugated plane. Steric hindrance may substantially affect the π-stacking distances and the density of the π-stacked backbones, decreasing the π-overlap area. Consequently, the bulky side chain in **PBDTTT-S** results in a low hole mobility of 4.56×10^{-4} $cm^2V^{-1}s^{-1}$, since the interchain hopping of carriers requires an overlap of the electron wavefunction of adjacent conjugated units on the polymer main chains.[35] In this regard, elongating the repeat unit along the backbone, by introducing a thiophene spacer, **PBDTDTTT-S-T**, can substantially increase the overlap area between adjacent conjugated chains and increase the hole mobility. As good charge transport is usually observed with polymers chains having a strong, ordered π-π stacking structure, **PBDTDTTT-S-T** exhibits a two-dimensionally ordered structure with a shorter π-stacking distance (GIXD) and, therefore, a hole mobility as high as 2.76×10^{-3} $cm^2V^{-1}s^{-1}$. In addition, shorter π-stacking distances tend to correlate with the higher charge-carrier mobilities. The density of π-stacked backbones within the active layer should further affect the efficiency of charge transport.[36,37]

The photovoltaic properties of the devices fabricated under optimal conditions are listed in **Table 2** and the corresponding *I-V* curves of these devices shown in **Figure 4**. For the BHJ OPV devices based on **PBDTDTTT-S-T**, a donor/acceptor (D/A) ratio of 1:1 was used in the active layer; For **PBDTTT-S** and **PBDTDTTT-S-T**, about 3% (DIO/DCB, v/v) DIO was added to the solution to get better photovoltaic performance.[15] Although

Table 2. Photovoltaic properties of PSCs based on the polymers as donor and $PC_{70}BM$ as acceptor under the illumination of AM1.5G, 100 mW/cm^2.

Polymers	Polymer: $PC_{70}BM$ [w/w]	Thickness [nm]	V_{oc} [V]	J_{sc} [mA/cm^2]	*FF* [%]	$PCE_{ave}(PCE_{max})$ [%]
PBDTTT-S	1:1.5	120	0.76	13.85	58.0	6.11 (6.36)
PBDTDTTT-S-T	1:1	110	0.69	16.35	66.3	7.48 (7.81)

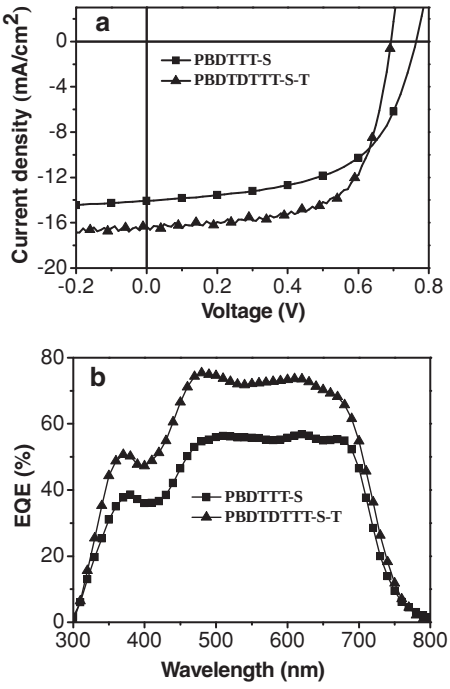

Figure 4. a) *I-V* characteristics of the devices with the structure of ITO/PEDOT:PSS/polymer:$PC_{70}BM$/Ca/Al under the illumination of AM 1.5G from a solar simulator (100 mW/cm^{-2}). b) EQE curves of the corresponding polymer solar cells.

the V_{oc} was slightly reduced by introducing the thiophene unit in the main chain, the J_{sc} and *FF* values of the BHJ OPV devices based on **PBDTDTTT-S-T** increased with the enlargement of conjugated area. The increase in mobility and better phase separation morphology after extending the conjugated area was the origin of the increased J_{sc} (increased from 13.85 to 16.35 mA cm^{-2}) and *FF* (from 58.0% to 66.3%), both of which contributed to the high efficiency of **PBDTDTTT-S-T**. Notably, the efficiencies of BHJ OPV devices based on **PBDTDTTT-S-T** were as high as 7.48% (average), with the highest efficiency being 7.81%, in comparison to 6.11% for the device based on **PBDTTT-S**. The external quantum efficiencies for the corresponding devices are shown in Figure 4b. The EQE exhibits two peaks coinciding with the absorption maxima of the blend. The EQE of the device based on **PBDTDTTT-S-T** approached over 70% at the energetically lower peak, i.e. at the absorption of maximum of the polymer.

In summary, **PBDTDTTT-S-T** was prepared using a stepwise modification process of the monomer structure following the design motif of extending the area of conjugation parallel to and normal to the polymer main chain axis. Two-dimensional conjugated systems have been obtained by enlarging the size of the donor unit and, therefore, increasing the extent π-π stacking and π-overlap area between the polymer main chains, resulting in high hole mobilities. The photovoltaic efficiencies of **PBDTDTTT-S-T**-based solar cells were as high as 7.81%, showing nearly a 25% increase after the simple modification. This effective and simple design motif can be widely used in other existing and new conjugated systems to optimize their

efficiencies. It is shown that extending the conjugation area in the monomer and, therefore, face-to-face packing between the polymer chains is an effective way to significantly increase photovoltaic efficiencies. A correlation between the molecular structure, thin film morphology, and photovoltaic properties of these conjugated polymers is established that provides guidance for the molecular design of new photovoltaic polymers.

Experimental Section

Materials: BDT and BDT-T monomers were purchased from Solarmer Materials Inc. All the other reagents and chemicals were purchased from commercial sources (J&K, Aldrich, Fluka) and used without further purification unless stated otherwise. Anhydrous tetrahydrofuran was distilled over sodium-benzophenone under nitrogen prior to use. HPLC grade DMF and toluene were used for polymerization.

Synthesis of Monomers and Polymers: 2-((2-hexyldecyl)sulfonyl)-4,6-di(thiophen-2-yl)thieno[3,4-b]thiophene (2). The synthesis began with 4,6-dibromo-2-((2-hexyldecyl)sulfonyl)thieno[3,4-b]thiophene (TT-S). To a solution of TT-S (2.34g, 4 mmol) and tributyl(2-thienyl)stannane (4.47g, 12 mmol) in Toluene (20 mL), DMF (4 mL), $Pd(PPh_3)_4$ (200 mg, 5 mol%) was added. The mixture was refluxed under a nitrogen atmosphere for 12 h. The liquid was extracted by ethyl ether three times. The combined organic phase was evaporated to remove the solvent under vacuum, and the residue was purified by silica gel chromatography using hexane:CH_2Cl_2 (1:1) as eluent to obtain compound 2. (2.13g, yield 90%) ^{1}H NMR ($CDCl_3$, 400MHz), δ (ppm): δ 7.84 (s, 1H), 7.37 (m, 2H), 7.31 (d, 1H), 7.22 (d, 1H), 7.11 (m, 2H), 3.12 (d, 2H), 2.06 (m, 1H), 1.1-1.5 (m, 24H), 0.81 (m, 6H). ^{13}C NMR ($CDCl_3$, 400MHz), δ (ppm): δ 146.96, 139.89, 135.25, 134.84, 134.79, 128.46, 128.33, 127.79, 126.33, 125.45, 125.38, 124.56, 124.19, 122.44, 33.44, 33.30, 31.85, 31.74, 29.65, 29.51, 29.31, 29.27, 27.85, 26.86, 26.01, 22.66, 17.54, 14.11, 14.05, 13.61.

4,6-bis(5-bromothiophen-2-yl)-2-((2-hexyldecyl)sulfonyl)thieno[3,4-b]thiophene (3). Under argon protection and dark against light, NBS (0.39g, 2.2mmol) was added to the solution of DMF (20mL) with compound 2 (1.18g, 2.0mmol) at 0 °C, the mixture was stirred for 5h at 0 °C, then the reactants were poured into the diluted solution of sodium thiosulfate and extracted by ethyl ether twice. The solvent was removed under vacuum and the coarse product was purified by silica gel chromatography using hexane:CH_2Cl_2 (2:1) as eluent to obtain compound 3 as orange solid (1.23g, yield 82%). ^{1}H NMR ($CDCl_3$, 400MHz), δ (ppm): δ 7.78 (s, 1H), 7.13 (d, 2H), 7.08 (d, 2H), 7.52 (d, 2), 6.91 (d, 2H), 3.20 (d, 2H), 2.08 (m, 1H), 1.55-1.2 (m, 24H), 0.87-0.82 (m, 6H). ^{13}C NMR ($CDCl_3$, 400MHz), δ (ppm): δ 147.68, 140.06, 136.02, 134.16, 134.06, 131.16, 125.93, 125.58, 124.44, 124.05, 121.68, 113.92, 113.53, 112.72, 60.95, 33.42, 33.28, 31.86, 31.75, 29.65, 29.52, 29.31, 29.28, 26.02, 25.12, 22.67, 22.62, 22.14, 14.12, 13.45.

Poly[((2-hexyldecyl)sulfonyl)-4,6-di(thiophen-2-yl)thieno[3,4-b]thiophene-2,6-diyl)-alt-(4,8-bis((2-ethylhexyl)oxy)benzo[1,2-b:4,5-b']dithiophene-2,6-diyl)] (**PBDTDTTT-S-T**): Amounts of 375.5 mg (0.5 mmol) of DTTT-S, 452 mg (0.5 mmol) of BDT-T, 25 mg $Pd(PPh_3)_4$ (5 mol%) and 10 mL of toluene were refluxed for 13 h under an argon atmosphere. The whole mixture was poured into methanol to afford a black solid. The purification process has been mentioned above (yield, 70%). ^{1}H NMR ($CDCl_3$, 400MHz), δ (ppm): δ 7.90-6.30 (m, br, 11H), 3.33-2.23 (m, br, 7H), 2.20-1.10 (m, br, 48H), 1.10-0.70 (m, br, 12H). Anal. Calcd for [$C_{64}H_{78}O_2S_9$]: C, 65.70; H, 6.89; O, 2.74; S, 24.67. Found: C, 65.41; H, 6.75. Weight average molecular weight (M_w) and polydispersity index (PDI) estimated from GPC are 125 kg/mol and 3.5, respectively.

General Methods: GIXD measurements were performed at Beamline 7.3.3, the Advanced Light Source, Lawrence Berkeley National Laboratory, Berkeley, CA. ^{1}H nuclear magnetic resonance (^{1}HNMR) and ^{3}C NMR spectra were obtained at Bruker DMX-400 spectrometer as solutions in $CDCl_3$. UV-visible absorption spectroscopy measurements were done using a Hitachi U-3100 UV-vis spectrophotometer. Atom Force Microscopy (AFM) was performed on a Nanoscope IIIA (Vecco) AFM in the tapping mode. Transmission electron microscopy (TEM) was performed using a JEOL 2200FS instrument at 160 kV accelerating voltage. The molecular weight of polymers was measured by GPC method, and polystyrene was used as the standard by using $CHCl_3$ as the eluent. TGA measurement was performed on a TA Instruments, Inc., TGA-2050. The electrochemical cyclic voltammetry was conducted on a CHI650D Electrochemical Workstation with Pt disk, Pt plate, and Ag/Ag^+ electrode as working electrode, counter electrode and reference electrode respectively, in a 0.1 M tetrabutylammonium hexafluorophosphate (Bu_4NPF_6) acetonitrile solution. The potential of Ag/Ag^+ reference electrode was internally calibrated by using the ferrocene/ferrocenium redox couple (Fc/Fc^+), which has a known energy level at –4.8 eV.[38]

Computational Study: In order to get an additional insight into the electronic structure of the polymers, density functional theory (DFT)[39] (using Gaussian 03 package[40] at the B3LYP/6-31G level of theory in vacuum)[41] was utilized to model the structural and electronic properties of relevant molecular structures. In particular, the HOMO and LUMO level positions and related electron distributions were calculated using three repeating units. The alkyl chains were replaced by methyl groups to keep the computational time within a reasonable range.

Polymer Solar Cell Device Fabrication: Polymer solar cell devices with the structure of ITO/PEDOT:PSS/polymer:$PCBM_{70}$/Ca/Al were fabricated under conditions as follows: After spin-coating a 30 nm layer of poly(3,4-ethylene dioxythiophene):poly(styrenesulfonate) onto a pre-cleaned indium-tin oxide (ITO) coated glass substrates, the polymer/$PC_{70}BM$ blend solution was spin-coated. The concentration of the polymer/$PC_{70}BM$ (1:1 or 1:1.5, weight ratio) blend solutions used in this work for spin-coating active layer was 10 mg/ml (based on the polymer weight concentration), and DCB was used as solvent, or 3% (v/v) DIO was used as additive to improve photovoltaic performance of the devices. The devices were completed by evaporating Ca/Al metal electrodes with area of 0.04 cm^2 defined by masks. The current-voltage curves are measured under 100 mW cm^{-2} standard AM 1.5 G spectrum using a XES-70S1 (SAN-EI ELECTRIC CO., LTD.) solar simulator (AAA grade, 70 mm × 70 mm photo-beam size). 2 × 2 cm Monocrystalline silicon reference cell (SRC-1000-TC-QZ) was purchased from VLSI Standards Inc. The mismatch between solar simulator and the standard solar spectrum has been considered.[42] The average PCE were obtained from more than 30 pieces of devices.

Supporting Information

Supporting Information is available from the Wiley Online Library or from the author.

Acknowledgements

J. Hou, L. Huo and Y. Li would like to acknowledge the financial support from National High Technology Research and Development Program 863 (2011AA050523), Chinese Academy of Sciences and NSFC (Nos.20874106, 51173189); T. P. Russell and F. Liu thank the DOE-supported Energy Frontier Research Center on Polymer-Based materials for Harvesting Solar Energy.

Received: March 9, 2012
Revised: April 15, 2012
Published online: May 31, 2012

[1] L. J. Huo, S. Q. Zhang, X. Guo, F. Xu, Y. F. Li, J. H. Hou, *Angew. Chem. Int. Ed.* **2011**, *50*, 9697.
[2] H. Y. Chen, J. H. Hou, S. Q. Zhang, Y. Y. Liang, G. W. Yang, Y. Yang, L. P. Yu, Y. Wu, G. Li, *Nat. Photon.* **2009**, *3*, 649.
[3] Y. Y. Liang, L. P. Yu, *Accounts. Chem. Res.* **2010**, *43*, 1227.
[4] C. M. Amb, S. Chen, K. R. Graham, J. Subbiah, C. E. Small, F. So, J. R. Reynolds, *J. Am. Chem. Soc.* **2011**, *133*, 10062.

[5] S. C. Price, A. C. Stuart, L. Q. Yang, H. X. Zhou, W. You, *J. Am. Chem. Soc.* **2011**, *133*.
[6] Z. C. He, C. M. Zhong, X. Huang, W. Y. Wong, H. B. Wu, L. W. Chen, S. J. Su, Y. Cao, *Adv. Mater.* **2011**, *23*, 4636.
[7] T. Y. Chu, J. P. Lu, S. Beaupre, Y. G. Zhang, J. R. Pouliot, S. Wakim, J. Y. Zhou, M. Leclerc, Z. Li, J. F. Ding, Y. Tao, *J. Am. Chem. Soc.* **2011**, *133*, 4250.
[8] G. Yu, J. Gao, J. C. Hummelen, F. Wudl, A. J. Heeger, *Science* **1995**, *270*, 1789.
[9] W. You, S. C. Price, A. C. Stuart, L. Q. Yang, H. X. Zhou, *J. Am. Chem. Soc.* **2011**, *133*, 4625.
[10] Y. Huang, M. J. Zhang, L. Ye, X. Guo, C. C. Han, Y. F. Li, J. H. Hou, *J. Mater. Chem.* **2012**, *22*, 5700.
[11] C. Kitamura, S. Tanaka, Y. Yamashita, *Chem. Mater.* **1996**, *8*, 570.
[12] J. H. Hou, H. Y. Chen, S. Q. Zhang, R. I. Chen, Y. Yang, Y. Wu, G. Li, *J. Am. Chem. Soc.* **2009**, *131*, 15586.
[13] Y. Huang, L. J. Huo, S. Q. Zhang, X. Guo, C. C. Han, Y. F. Li, J. H. Hou, *Chem. Commun.* **2011**, *47*, 8904.
[14] G. Li, V. Shrotriya, J. S. Huang, Y. Yao, T. Moriarty, K. Emery, Y. Yang, *Nature Materials* **2005**, *4*, 864.
[15] J. Peet, J. Y. Kim, N. E. Coates, W. L. Ma, D. Moses, A. J. Heeger, G. C. Bazan, *Nature Materials* **2007**, *6*, 497.
[16] Y. Yao, J. Hou, Z. Xu, G. Li, Y. Yang, *Adv. Funct. Mater.* **2007**, *18*, 1783.
[17] C. Piliego, T. W. Holcombe, J. D. Douglas, C. H. Woo, P. M. Beaujuge, J. M. J. Frechet, *J. Am. Chem. Soc.* **2010**, *132*, 7595.
[18] M. C. Scharber, M. Koppe, J. Gao, F. Cordella, M. A. Loi, P. Denk, M. Morana, H. J. Egelhaaf, K. Forberich, G. Dennler, R. Gaudiana, D. Waller, Z. G. Zhu, X. B. Shi, C. J. Brabec, *Adv. Mater.* **2010**, *22*, 367.
[19] H. Y. Chen, J. H. Hou, A. E. Hayden, H. Yang, K. N. Houk, Y. Yang, *Adv. Mater.* **2010**, *22*, 371.
[20] X. L. Feng, V. Marcon, W. Pisula, M. R. Hansen, J. Kirkpatrick, F. Grozema, D. Andrienko, K. Kremer, K. Mullen, *Nature Materials* **2009**, *8*, 421.
[21] W. Pisula, Z. Tomovic, C. Simpson, M. Kastler, T. Pakula, K. Mullen, *Chem. Mater.* **2005**, *17*, 4296.
[22] M. Berggren, O. Inganas, G. Gustafsson, J. Rasmusson, M. R. Andersson, T. Hjertberg, O. Wennerstrom, *Nature* **1994**, *372*, 444.
[23] J. A. Letizia, M. R. Salata, C. M. Tribout, A. Facchetti, M. A. Ratner, T. J. Marks, *J. Am. Chem. Soc.* **2008**, *130*, 9679.
[24] D. E. Janzen, M. W. Burand, P. C. Ewbank, T. M. Pappenfus, H. Higuchi, D. A. da Silva, V. G. Young, J. L. Bredas, K. R. Mann, *J. Am. Chem. Soc.* **2004**, *126*, 15295.
[25] J. H. Hou, Z. A. Tan, Y. Yan, Y. J. He, C. H. Yang, Y. F. Li, *J. Am. Chem. Soc.* **2006**, *128*, 4911.
[26] M. C. Scharber, D. Wuhlbacher, M. Koppe, P. Denk, C. Waldauf, A. J. Heeger, C. L. Brabec, *Adv. Mater.* **2006**, *18*, 789.
[27] Y. Y. Liang, D. Q. Feng, Y. Wu, S. T. Tsai, G. Li, C. Ray, L. P. Yu, *J. Am. Chem. Soc.* **2009**, *131*, 7792.
[28] D. A. Chen, A. Nakahara, D. G. Wei, D. Nordlund, T. P. Russell, *Nano Lett.* **2011**, *11*, 561.
[29] J. T. Rogers, K. Schmidt, M. F. Toney, E. J. Kramer, G. C. Bazan, *Adv. Mater.* **2011**, *23*, 2284.
[30] T. Agostinelli, T. A. M. Ferenczi, E. Pires, S. Foster, A. Maurano, C. Muller, A. Ballantyne, M. Hampton, S. Lilliu, M. Campoy-Quiles, H. Azimi, M. Morana, D. D. C. Bradley, J. Durrant, J. E. Macdonald, N. Stingelin, J. Nelson, *J. Polym. Sci. Pol. Phys* **2011**, *49*, 717.
[31] G. Yu, P. R. Thomas, *American Physical Society March Meeting,* **2011**, March 21-25, 2011, abstract #C1.007.
[32] M. Morana, H. Azimi, G. Dennler, H. J. Egelhaaf, M. Scharber, K. Forberich, J. Hauch, R. Gaudiana, D. Waller, Z. H. Zhu, K. Hingerl, S. S. van Bavel, J. Loos, C. J. Brabec, *Adv. Funct. Mater.* **2010**, *20*, 1180.
[33] G. G. Malliaras, J. R. Salem, P. J. Brock, C. Scott, *Phys. Rev. B* **1998**, *58*, 13411.
[34] H. C. F. Martens, H. B. Brom, P. W. M. Blom, *Phys. Rev. B* **1999**, *60*, R8489.
[35] J. L. Bredas, R. Silbey, *Science* **2009**, *323*, 348.
[36] R. A. Street, J. E. Northrup, A. Salleo, *Phys. Rev. B* **2005**, *71*, 165202.
[37] P. M. Beaujuge, W. Pisula, H. N. Tsao, S. Ellinger, K. Mullen, J. R. Reynolds, *J. Am. Chem. Soc.* **2009**, *131*, 7514.
[38] X. W. Zhan, Y. Q. Liu, X. Wu, S. Wang, D. B. Zhu, *Macromolecules.* **2002**, *35*, 2529.
[39] R. G. Parr, Y. Weitao, *Density Functional Theory of Atoms and Molecules*; Oxford University Press: New York **1989**.
[40] M. J. Frisch, G. W. Trucks, H. B. Schlegel, G. E. Scuseria, M. A. Robb, J. R. Cheeseman, J. A. Montgomery, Jr., T. Vreven, K. N. Kudin, J. C. Burant, J. M. Millam, S. S. Iyengar, J. Tomasi, V. Barone, B. Mennucci, M. Cossi, G. Scalmani, N. Rega, G. A. Petersson, H. Nakatsuji, M. Hada, M. Ehara, K. Toyota, R. Fukuda, J. Hasegawa, M. Ishida, T. Nakajima, Y. Honda, O. Kitao, H. Nakai, M. Klene, X. Li, J. E. Knox, H. P. Hratchian, J. B. Cross, V. Bakken, C. Adamo, J. Jaramillo, R. Gomperts, R. E. Stratmann, O. Yazyev, A. J. Austin, R. Cammi, C. Pomelli, J. W. Ochterski, P. Y. Ayala, K. Morokuma, G. A. Voth, P. Salvador, J. J. Dannenberg, V. G. Zakrzewski, S. Dapprich, A. D. Daniels, M. C. Strain, O. Farkas, D. K. Malick, A. D. Rabuck, K. Raghavachari, J. B. Foresman, J. V. Ortiz, Q. Cui, A. G. Baboul, S. Clifford, J. Cioslowski, B. B. Stefanov, G. Liu, A. Liashenko, P. Piskorz, I. Komaromi, R. L. Martin, D. J. Fox, T. Keith, M. A. Al-Laham, C. Y. Peng, A. Nanayakkara, M. Challacombe, P. M. W. Gill, B. Johnson, W. Chen, M. W. Wong, C. Gonzalez, J. A. Pople, Gaussian 03, Revision B.03, I. P. Gaussian, PA, **2003**.
[41] A. D. Becke, *J. Chem. Phys.* **1993**, *98*, 5648.
[42] V. Shrotriya, G. Li, Y. Yao, T. Moriarty, K. Emery, Y. Yang, *Adv. Funct. Mater.* **2006**, *16*, 2016.